Available online at www.sciencedirect.com
ScienceDirect
Atmospheric Environment 41 (2007) 465–479
ATMOSPHERIC ENVIRONMENT
www.elsevier.com/locate/atmosenv

Bayesian inference for source determination with applications to a complex urban environment

Andrew Keats[a], Eugene Yee[b,*], Fue-Sang Lien[a]

[a]*Department of Mechanical Engineering, University of Waterloo, Waterloo, Ont., Canada N2L 3G1*
[b]*Defence R&D Canada—Suffield, P.O. Box 4000, Medicine Hat, AB, Canada T1A 8K6*

Received 28 May 2006; received in revised form 21 August 2006; accepted 22 August 2006

Abstract

The problem of determining the source of an emission from the limited information provided by a finite and noisy set of concentration measurements obtained from real-time sensors is an ill-posed inverse problem. In general, this problem cannot be solved uniquely without additional information. A Bayesian probabilistic inferential framework, which provides a natural means for incorporating both errors (model and observational) and prior (additional) information about the source, is presented. Here, Bayesian inference is applied to find the posterior probability density function of the source parameters (location and strength) given a set of concentration measurements. It is shown how the source–receptor relationship required in the determination of the likelihood function can be efficiently calculated using the adjoint of the transport equation for the scalar concentration. The posterior distribution of the source parameters is sampled using a Markov chain Monte Carlo method. The inverse source determination method is validated against real data sets acquired in a highly disturbed flow field in an urban environment. The data sets used to validate the proposed methodology include a water-channel simulation of the near-field dispersion of contaminant plumes in a large array of building-like obstacles (Mock Urban Setting Trial) and a full-scale field experiment (Joint Urban 2003) in Oklahoma City. These two examples demonstrate the utility of the proposed approach for inverse source determination.

Keywords: Adjoint equations; Bayesian inference; Dispersion modelling; Source determination; Urban flows

1. Introduction

Determining the emission source of a contaminant released into the atmosphere has recently become a topic of intensive research because it carries important implications for both emergency and environmental management. The US Department of Homeland Security envisions using city-wide detector networks capable of sensing chemical, biological or radiological (CBR) emissions as a tool for mitigating potential acts of terrorism involving the release of CBR agents. Using a robust source determination methodology in conjunction with CBR detector measurements would provide emergency services with valuable additional information about the location and nature of a threat. On wider spatial and temporal scales, the problem of environmental contamination warrants the use of a source determination methodology in a number of settings. Above ground, industrial sites issuing

*Corresponding author. Tel.: +1 403 544 4605; fax: +1 403 544 3388.
E-mail address: eugene.yee@drdc-rddc.gc.ca (E. Yee).

1352-2310/$ - see front matter © 2006 Elsevier Ltd. All rights reserved.
doi:10.1016/j.atmosenv.2006.08.044

spurious emissions can be pinpointed (Skiba, 2003; Goyal et al., 2005), and regional sources of air pollution identified (Lin and Chang, 2002). Below ground, aquifer contamination history can be inferred (Aral et al., 2001; Michalak and Kitanidis, 2003). Another application of global importance is the enforcement of the Comprehensive Test Ban Treaty (CTBT). A world-wide network of radionuclide detectors is in place as a verification tool and can be used to potentially isolate the location of clandestine nuclear testing (Geer, 1996; Hourdin and Issartel, 2000).

Research devoted to estimating the strength (emission rate) of a contaminant source using a fixed network of concentration measurements has been undertaken by Wilson and Shum (1992), who estimated the rate of ammonia volatilization from field plots using a Lagrangian trajectory model, and also by Flesch et al. (1995), who used a backward-time Lagrangian Stochastic model to estimate the emission rate of a sustained surface area source in horizontally homogeneous turbulence. A related problem is that of characterizing the strengths of a variety of sources whose locations are known a priori. Lin and Chang (2002) used backward trajectories to examine the relative contributions of various anthropogenic sources to the ozone formation potential at various receptor sites in southern Taiwan, and Skiba (2003) used an adjoint pollution transport model to estimate the emission rates of various industrial plants in Mexico.

Additional research has focussed on estimating the source location, rather than its strength. Nehorai et al. (1995) and Jeremić and Nehorai (2000) determined the physical location of a point source using a static network of detectors measuring concentration over time. They modelled the dispersion of the contaminant exclusively using a diffusion mechanism, and estimated the location of the source using a maximum-likelihood method. Matthes et al. (2005) further refined the solution to the problem by taking advection into account, and used an analytical solution to the advection-diffusion equation in conjunction with a least-squares approach to estimate the source location. All of the aforementioned approaches assume idealized, undisturbed homogeneous flow fields, and treat the problem in an optimization framework using Monte Carlo or gradient-based methods. In contrast, the present work accounts for highly disturbed flow fields present in built-up environments and must rely on numerical solutions to the dispersion equations.

The simultaneous estimation of both the location and strength of the source was performed on a global scale by Pudykiewicz (1998), who considered the problem of determining the source of a radioactive tracer. He recognized the problem as probabilistic in nature, and solved adjoint dispersion equations backwards in time in a global context. However, he mistakenly interpreted the solution to the adjoint equations as representing a probability density function (PDF) of the source location. In Section 2.2.1 we explain why this interpretation is invalid. Robertson (2004) used a similar strategy in that a weighted combination of 'influence functions' (the output of the adjoint dispersion equations) was used to narrow the set of possible source locations, while determining the contribution of a prospective source region to the concentration level at a detector. Sohn et al. (2002) addressed the problem of characterizing the location, strength and duration of an indoor release using a Bayesian framework. They precomputed detector data using an indoor mutizone air flow and contaminant transport model which treats buildings as a collection of well-mixed zones (rooms), a simplification which cannot be made in the present work where detailed flow information is required to calculate dispersion. Chow et al. (2005), Kosovic et al. (2005) and Rapley et al. (2005) recognized that source reconstruction may be undertaken using a combination of Bayesian inference and Markov chain Monte Carlo (MCMC) methods, but did not implement adjoint dispersion equations for quickly computing source-receptor relationships (the expected detector concentrations for a given source configuration). As a result, their calculations were computationally intensive (witness Chow et al. (2005) who reported an example of source reconstruction requiring 13,056 CPU hours for computation of the source-receptor relationships needed for the inversion). Recent work of Hsieh et al. (2005), Keats et al. (2006), Yee (2006) and Yee et al. (2006b) has addressed this problem by using the adjoint advection-diffusion equation in conjunction with MCMC methods to perform the computations efficiently.

When a limited amount of detector data is available (practically speaking, detectors cannot be placed at every point in the domain), determining the source of a contaminant dispersed in the atmosphere is an ill-posed inverse problem. If the number of sources is known a priori, this problem becomes one of parameter estimation; we are given a theoretical model relating source characteristics to

the expected concentrations at the detectors that is subject to model errors and actual concentration data measured by a small number of detectors that are subject to observational errors (measurement noise). Considering the problem in this manner, it becomes imperative to use a probabilistic framework to obtain a solution. Using an optimization approach is insufficient in this context, as it fails to provide information about the source parameter probabilities encapsulated in the region surrounding the critical point, and the choice of metric used to evaluate the objective function is arbitrary. Probability theory avoids this problem by obtaining the solution rationally in a way consistent with all available prior information, and presenting it as a holistic 'state of information' about the source parameters. Starting with logically consistent assumptions about the nature of the uncertainties involved in both experimental and modelled detector concentrations, applying probability theory as a form of extended logic (Cox, 1946; Jaynes, 2003) yields an honest estimate of the source parameters, including their degree of uncertainty.

The main objective of this paper is to show how Bayesian inference can be applied to solve a source determination problem in a consistent and computationally efficient way through the combined use of adjoint dispersion equations and MCMC methods. Section 2 formulates the problem for a time-dependent transient release (as well as the special case of a steady continuous release) from a point source and explains the rationale behind using the adjoint equation and MCMC approaches. The methodology is validated using two different test cases in Sections 3 and 4, in which we simultaneously estimate the source location and strength for dispersion experiments performed in built-up environments.

2. Problem formulation and solution

The use of probability theory to formulate the source determination problem is sanctioned by the fact that the rules of probability theory form a 'calculus of inductive logic' (or inference) which allows us to manipulate proposals whose plausibility can be represented by a real number (e.g., $P \in [0,1]$), rather than simply by True or False (e.g., 0 or 1). Cox (1946) began with simple desiderata:

(1) degrees of plausibility can be represented using real numbers,

(2) the calculus should be consistent (viz., different methods of calculation should yield the same results)

and showed that the rules of probability calculus are equivalent to the rules for conducting inference (in essence, reasoning from incomplete information). Phrasing the source determination problem as one of inference allows us to formulate it in a consistent manner, based on all of the relevant information available. Maintaining a focus on the 'information content' of the problem ensures that no unjustified assumptions about the nature of the source parameters are made, yielding forthright estimates of their uncertainty. Exclusively using conditional probabilities in the problem formulation emphasizes the relationships between hypotheses ('|' means 'given' or 'conditional on'), as well as the fact that all information is contextual (hypotheses to the right of '|' provide the context, so I below is used as a generic label for all the hypotheses underlying the background context).[1]

Consider a vector of parameters, $\mathbf{m}$, which describe the properties of a transient point source:

$$\mathbf{m} = (x_s, y_s, z_s, q_s, t_{on}, t_{off}), \tag{1}$$

where $\{x_s, y_s, z_s\}$ represent the spatial location of the source, q_s is its strength (of dimension $[MT^{-1}]$), and $\{t_{on}, t_{off}\}$ are turn-on and turn-off times. Bayes' theorem provides a way to manipulate the conditional PDFs of the vector of source parameters $\mathbf{m}$, the concentration data D, and background information I:

$$\underbrace{P(\mathbf{m}|D,I)}_{\text{Posterior}} = \frac{\overbrace{P(m|I)}^{\text{Prior}}\overbrace{P(D|\mathbf{m},I)}^{\text{Likelihood}}}{\underbrace{P(D|I)}_{\text{Evidence}}}. \tag{2}$$

Using PDFs in the problem formulation allows us to account for uncertainties in our observational and model concentration data. It also provides a way to account for the fact that although many different source configurations may be plausible, some will be more probable than others. However, while the Bayesian approach provides the overall framework for solving this inverse problem, other techniques are required for our calculations to be of practical use (viz., both timely and sufficiently

[1] All probabilities are necessarily conditional because probabilities do not make sense until the evidence upon which they are based is stated.

representative of our 'state of knowledge' of the source). Calculating the theoretical source-receptor relationship (the modelled mean concentration expected by a detector for a given source configuration) is rapidly accomplished using the adjoint advection–diffusion equation, which is described in Section 2.2. Furthermore, the posterior PDF, whose dimensionality may be high, must be sampled. This is accomplished using the MCMC method, as presented in Section 2.3. Combining Bayesian inference with the adjoint and MCMC techniques results in an efficient and effective method for determining the source of a dispersion.

2.1. Bayesian formulation

The full solution to the source determination problem is the posterior PDF, which represents the probability that the source parameters $\mathbf{m}$ take certain values, given (i) a set of concentration measurements D and (ii) any other background information I that is applicable to the problem. In order to be of practical use, this PDF must be marginalized for each source parameter m_i, and suitable summary statistics (e.g., the mean and standard deviations, $\overline{m_i}$ and σ_{m_i}) must be extracted.

Using the MCMC method, we are able to draw samples from the posterior PDF without knowing the normalization constant, so a simplified version of Eq. (2) is used:

$$\underbrace{P(\mathbf{m}|D,I)}_{\text{Posterior}} \propto \underbrace{P(\mathbf{m}|I)}_{\text{Prior}}\underbrace{P(D|\mathbf{m},I)}_{\text{Likelihood}}. \tag{3}$$

This avoids the need to calculate the evidence term (see Eq. (2)), a complicated multidimensional integral required for normalization. The posterior distribution is proportional to the product of the likelihood and prior distributions, which are formulated in the following section.

2.1.1. Assignment of the likelihood function

The likelihood function expresses the following: given that the source is described by the parameters $\mathbf{m}$, provide the probability that an array of detectors observes a certain set of concentrations D. This probability quantifies the likelihood of the discrepancy between the measured concentrations D and a corresponding set of modelled concentrations, R, termed the theoretical source-receptor relationship. R_i is the concentration value that detector i would theoretically measure if the source were characterized correctly by the parameters $\mathbf{m}$, and is determined by a mathematical model of atmospheric dispersion.

The discrepancy between the measured and modelled concentrations at the ith detector, D_i and R_i, arises from (at least) two sources: measurement and model error. First, consider that the measured mean concentration is subject to a noise component, e_i^{meas}:

$$D_i = D_{\text{true},i} + e_i^{\text{meas}}, \tag{4}$$

where $D_{\text{true},i}$ is the (unknown) true value of the mean concentration at the ith detector. In this work, we assume the noise e_i to be normally distributed, although other distributions such as the lognormal distribution can also be used (Goyal et al., 2005). Nevertheless, Sohn et al. (2002) have performed similar analyses (source identification) using Gaussian distributions, which we adopt here. Similarly, the discrepancy e_i^{model} between the modelled and true concentrations, is assumed also to be normally distributed:

$$R_i = D_{\text{true},i} + e_i^{\text{model}}. \tag{5}$$

Both noise components are assumed to have a mean of zero and variances of $\sigma_{D,i}^2$ and $\sigma_{T,i}^2$, respectively.[2] Furthermore, the measurement and model errors for any detector are statistically independent, as are these errors across different detectors. The measurement error is then codified as

$$P(D|D_{\text{true}},I) \propto \exp\left[-\frac{1}{2}\sum_i \frac{(D_i - D_{\text{true},i})^2}{\sigma_{D,i}^2}\right], \tag{6}$$

which represents the probability that the observed data are measured as D when the true values are

[2]When provided with only the mean and variance of the noise e_i, the principle of maximum entropy (Jaynes, 2003) or MAXENT principle asserts that the maximally non-committal (least informative) PDF for the noise (effectively the likelihood) is the Gaussian distribution. The entropy of the PDF of the noise is a measure of the size of the basic support set of the distribution or 'volume' occupied by the sensibly probable noise values. Choosing a distribution for the noise that provides the largest support set permitted by the available information allows the largest range of possible variations in the noise values consistent with that information, implying the most conservative estimates for these values. Assigning a Gaussian distribution for the noise using the MAXENT principle makes no statement about the true (unknown) sampling distribution of the measurement or model errors; rather, it simply represents a maximally uninformative state of knowledge, a state of knowledge that reflects what the observer knows about the true noise in the data (namely, the mean and variance of the noise, with all other properties of the noise being irrelevant to the inference since these are unknown to the observer).

actually D_{true}; the model error is codified as

$$P(D_{\text{true}}|\mathbf{m}, I) \propto \exp\left[-\frac{1}{2}\sum_i \frac{(D_{\text{true},i} - R_i(\mathbf{m}))^2}{\sigma_{T,i}^2}\right], \quad (7)$$

which states the probability that the true data are predicted by the model for the source-receptor relationship when the source parameters are $\mathbf{m}$. The likelihood is then obtained by marginalizing the joint PDF of D and D_{true} with respect to D_{true}:

$$P(D|\mathbf{m}, I) = \int_{\text{all } D_{\text{true}}} P(D|D_{\text{true}}, I)P(D_{\text{true}}|\mathbf{m}, I)\mathrm{d}D_{\text{true}}. \quad (8)$$

Evaluating the integral of Eq. (8) yields the likelihood:

$$P(D|\mathbf{m}, I) \propto \exp\left[-\frac{1}{2}\sum_i \frac{(D_i - R_i(\mathbf{m}))^2}{\sigma_{D,i}^2 + \sigma_{T,i}^2}\right]. \quad (9)$$

Assuming that we know D, σ_D and σ_T, calculating $R_i(\mathbf{m})$ for various $\mathbf{m}$ provides $P(D|\mathbf{m}, I)$.

2.1.2. Assignment of the prior probability

The prior probability encompasses any information known about the source parameters prior to the receipt of the concentration data. For example, if the effects of a toxic gas were to be qualitatively observed in some region of space, e.g., $\{x, y\} \subset \Omega$, then the value of the prior probability could be increased in this region according to the reliability of the observations.

In the present research, it is assumed that nothing is known about the source parameters beforehand, and that the parameters are independent, in that knowledge of one parameter does not imply anything about the others. According to the principle of maximum entropy (which reduces to Laplace's principle of indifference in this case), the PDF whose distribution expresses complete ignorance about the parameter values is flat (Jaynes, 2003); therefore, the prior PDF is assigned a uniform distribution over the domain of definition $\Re$ for the source parameters:

$$P(\mathbf{m}|I) = \text{constant}, \quad \mathbf{m} \in \Re. \quad (10)$$

Of course, any PDF must integrate to unity, which is accomplished in this case by bounding the parameters $\mathbf{m}$. For a bounded computational domain $\Re$, we have $(x_s, y_s, z_s, q_s, t_{on}, t_{off}) \in \Re$; for example, the source strength q_s is assumed to be greater than zero but less than some practical upper limit. The prior probability is also used to discount the possibility that the source lies within a building. It is set to zero in all of the within-building regions.

2.1.3. The posterior probability density function

Since the prior is constant, the posterior PDF is essentially proportional to the likelihood:

$$P(\mathbf{m}|D, I) \propto P(\mathbf{m}|I)P(D|\mathbf{m}, I) \propto I(\mathbf{m} \in \Re)\exp\left[-\frac{1}{2}\sum_i \frac{(D_i - R_i(\mathbf{m}))^2}{\sigma_{D,i}^2 + \sigma_{T,i}^2}\right], \quad (11)$$

where $I(\cdot)$ denotes the indicator function.

2.2. Source-receptor relationship

Efficiently calculating the source-receptor relationship $R(\mathbf{m})$ is crucial to the practical success of the source determination methodology. Under a brute-force approach, the forward advection–diffusion Eq. (13) must be solved for every required combination of source parameters $\mathbf{m}$ (of which there may be potentially hundreds of millions). This approach yields an entire concentration field when only a limited set of modelled concentration measurements are required. In this paper, we adopt an adjoint approach in which the adjoint advection–diffusion equation is solved only once for each detector, and the resulting conjugate concentration field is used to rapidly calculate the expected detector concentration for every required combination of source parameters. Solving the adjoint advection–diffusion equation requires approximately the same computational time as the forward advection–diffusion equation.

Consider a transient point source distribution Q $[ML^{-3}T^{-1}]$ which releases material at a steady rate of q_s $[MT^{-1}]$ and whose turn-on and turn-off times are t_{on} and t_{off}:

$$Q = q_s\delta(\mathbf{x} - \mathbf{x}_s)[H(t - t_{on}) - H(t - t_{off})], \quad (12)$$

where $\delta(\cdot)$ and $H(\cdot)$ are the Dirac delta and Heaviside unit step functions, respectively; and, $\mathbf{x}_s = \{x_s, y_s, z_s\}$ is the (point) source location. The advection–diffusion equation,

$$\frac{\partial C}{\partial t} + \mathbf{u}\cdot\nabla C - \nabla\cdot(K\nabla C) = Q$$
$$\text{subject to} \quad \nabla_{\mathbf{n}} C = 0 \quad \text{at } \partial\Omega,$$
$$C(\mathbf{x}, t = t_{on}) = 0 \quad (13)$$

models the release of the source Q over a space-time domain $\Omega \times [0, T]$ through the time evolution of the

concentration field, C. Here, C $[ML^{-3}]$ denotes a Reynolds-averaged (or, mean) concentration and the components of $\mathbf{u}$ are Reynolds-averaged (or, mean) wind velocities in the x, y, z directions. K is an eddy diffusivity used to model the turbulent scalar fluxes, and $\partial\Omega$ is the boundary of the spatial domain. The vector $\mathbf{n}$ refers to the boundary-normal direction, and $\nabla_{\mathbf{n}}$ is a directional derivative.

Next, consider the modelled concentration measurement at the ith detector, R_i. This specific value is a linear functional of the concentration field, C, and is determined by the inner product of C and a 'detector response function', h $[L^{-3}T^{-1}]$, for a specific location and measurement time:

$$R_i = \langle C, h\rangle \equiv \int_0^T \mathrm{d}t \int_\Omega Ch \,\mathrm{d}\Omega, \tag{14}$$

where $h = h(\mathbf{x}-\mathbf{x}_r,\ t-t_r)$ for a detector which measures the concentration at location $\mathbf{x}_r$ and time t_r. The function h acts as a space-time filter and would be, e.g., a delta function in both space and time for an ideal detector with infinite spatial and temporal resolving power. According to the duality relationship, R_i can also be obtained using the inner product of the conjugate concentration field C^* $[L^{-3}]$ and the source function Q:

$$R_i = \langle Q, C^*\rangle \equiv \int_0^T \mathrm{d}t \int_\Omega QC^* \mathrm{d}\Omega, \tag{15}$$

where the C^* field evolves according to the adjoint advection–diffusion equation:

$$-\frac{\partial C^*}{\partial t} - \mathbf{u}\cdot\nabla C^* - \nabla\cdot(K\nabla C^*) = h,$$
$$\text{subject to}\quad K\nabla_{\mathbf{n}}C^* + \mathbf{u}\cdot\mathbf{n}C^* = 0 \text{ at } \partial\Omega,$$
$$C^*(\mathbf{x}, t = t_r) = 0. \tag{16}$$

The general procedure for obtaining the adjoint of a linear operator is outlined by Estep (2004), and is briefly summarized below for the present case. The adjoint Eq. (16) is obtained by first multiplying the forward advection–diffusion Eq. (13) by a test function, C^*, and integrating this result over the space-time domain:

$$\int_0^T \mathrm{d}t \int_\Omega C^* \frac{\partial C}{\partial t}\,\mathrm{d}\Omega + \int_0^T \mathrm{d}t \int_\Omega C^*\mathbf{u}\cdot\nabla C\,\mathrm{d}\Omega - \int_0^T \mathrm{d}t \int_\Omega C^*\nabla\cdot(K\nabla C)\,\mathrm{d}\Omega = \int_0^T \mathrm{d}t \int_\Omega C^* Q\,\mathrm{d}\Omega. \tag{17}$$

Integrating by parts and taking advantage of the divergence theorem where applicable, the derivative terms can be rearranged to yield an expression which is compatible with

$$\langle C, h\rangle = \langle Q, C^*\rangle + \text{boundary terms} \tag{18}$$

and which obeys the boundary conditions associated with the forward problem. The term h manifests itself in this expression as the left-hand-side of Eq. (16) and can be extracted by inspection. Boundary conditions for the adjoint advection-diffusion equation are chosen such that the boundary terms of Eq. (18) vanish, resulting in the duality relationship between C and C^*,

$$\langle C, \mathbf{L}^*C^*\rangle = \langle \mathbf{L}C, C^*\rangle$$
$$\text{or}\quad \langle C, h\rangle = \langle Q, C^*\rangle. \tag{19}$$

The linear operators $\mathbf{L}$ and $\mathbf{L}^*$ are defined by

$$\mathbf{L}(\cdot) \equiv \frac{\partial}{\partial t}(\cdot) + \mathbf{u}\cdot\nabla(\cdot) - \nabla\cdot(K\nabla(\cdot)),$$
$$\Rightarrow \mathbf{L}(C) = Q, \tag{20}$$

$$\mathbf{L}^*(\cdot) \equiv -\frac{\partial}{\partial t}(\cdot) - \mathbf{u}\cdot\nabla(\cdot) - \nabla\cdot(K\nabla(\cdot)),$$
$$\Rightarrow \mathbf{L}^*(C^*) = h. \tag{21}$$

The inner product of Eq. (19) can be rapidly calculated in order to find the concentration at a detector for any choice of Q using the value of the C^* field at the location of the point source. For a line, area or volume source, this calculation would be more involved, but still significantly simpler than re-solving Eq. (13) for a new source term.

In practice, detectors do not obtain concentration readings continuously; rather, they measure for a period of time and provide the average concentration over that period. Therefore, the concentration information at detector i typically takes the form of a time series, with each data point centered around a time of measurement, $t_j^{(i)}$. The modelled concentration read by detector i during time period j is denoted by $C_i^{(j)}$. Fig. 1 shows how a smooth (theoretical) concentration curve might be sampled by a detector.

It is necessary to solve Eq. (16) once for every possible (i,j) in order to find $C^*{}_i^{(j)}$. Substituting the assumed source distribution of Eq. (12) into the duality relationship of Eq. (19), one obtains the

source-receptor relationship:

$$R_i^{(j)}(\mathbf{m}) = q_s \int_{t_{on}}^{\min\left(t_j^{(i)}, t_{off}\right)} C_i^{*(j)}(\mathbf{x}_s, t_s) \mathrm{d}t_s, \tag{22}$$

where $C^{*(j)}_i$ is a time-varying conjugate concentration field corresponding to the measurement taken by detector i during time period $t_j^{(i)}$, and $R_i^{(j)}(\mathbf{m})$ is the averaged concentration that detector i would expect to have measured during $t_j^{(i)}$ if the source was correctly characterized by $\mathbf{m}$. The total number of unsteady C^* fields that need to be generated is equal to the product of the number of detectors (indexed by i) multiplied by the number of time intervals $t_j^{(i)}$ sampled at detector i. Finally, it is important to note that calculating the posterior distribution involves a summation over all possible (i, j):

$$P(\mathbf{m}|D, I) \propto I(\mathbf{m} \in \mathfrak{R}) \exp\left[-\frac{1}{2}\sum_{i,j} \frac{\left(C_i^{(j)} - R_i^{(j)}(\mathbf{m})\right)^2}{\sigma_{D,i,j}^2 + \sigma_{T,i,j}^2}\right]. \tag{23}$$

2.2.1. Continuous releases

The problem of a point source which releases material continuously in time into a statistically stationary wind field is a special case of the more general formulation presented above. Here, we consider a point source of the form:

$$Q = q_s \delta(\mathbf{x} - \mathbf{x}_s), \tag{24}$$

which is a special case of Eq. (12) for $t_{on} \to -\infty$ and $t_{off} \to \infty$ with a temporal integration effected over all time. The steady-state forward and adjoint advection–diffusion equations are obtained by integrating Eqs. (13) and (16), respectively, over all time:

$$\mathbf{u} \cdot \nabla C - \nabla \cdot (K \nabla C) = Q, \tag{25}$$

$$-\mathbf{u} \cdot \nabla C^* - \nabla \cdot (K \nabla C^*) = h. \tag{26}$$

The units of C^* and h become $[TL^{-3}]$ and $[L^{-3}]$, respectively, and the duality relationship, Eq. (19), remains applicable. Thus, the source-receptor relationship is calculated using:

$$R_i(\mathbf{m}) = q_s C_i^*(x_s, y_s, z_s), \tag{27}$$

where the set of parameters has been reduced to $\mathbf{m} = \{x_s, y_s, z_s, q_s\}$.

In this context it is convenient to demonstrate how the C^* field may also be interpreted as a 'region of influence'; an area in space where a source may possibly have contributed to the concentration reading observed at the detector. For this reason, detectors which measure zero concentration can provide useful information by narrowing the set of possible source locations. The relevance of C and C^* fields to a continuous release problem is illustrated in Fig. 2. Note that the region of influence $(C_2^* \cap C_3^* \backslash C_1^*)$ is significantly smaller than the size of the plume, C. C_1^* is excluded from the region of influence because according to the shape of C, detector d_1 measures zero concentration.

Some authors (Pudykiewicz, 1998; Robertson, 2004) use these regions of influence to isolate the source location but it is important to point out that the probability of the source lying in a given region

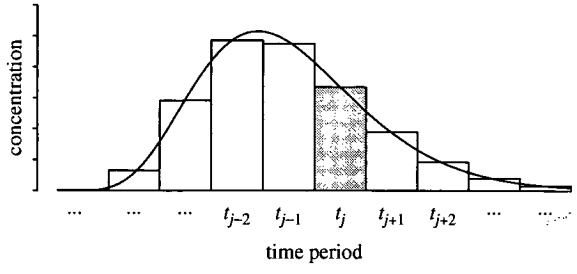

Fig. 1. A detector measures an average value of the concentration over time period j, resulting in a series of concentration readings at times t_j.

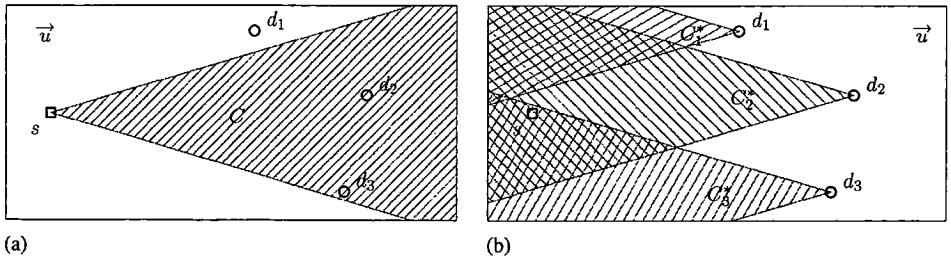

Fig. 2. Illustration showing the relationships between the source, detectors, C field, and C^* fields for a 2D problem layout with one source (denoted by s) and three detectors (d_1, d_2, d_3). (a) Forward problem and (b) adjoint problem.

is not proportional to the value of the C^* field in that region. For example, consider the C^* field generated from a single detector location. A source lying anywhere within the non-zero area of the C^* field could have contributed to a concentration measurement at the detector, depending on its emission strength.

2.3. Sampling using Markov chain Monte Carlo method

Although the value of the posterior distribution can be obtained directly to within a constant of proportionality, this calculation is nevertheless computationally expensive when conducted millions or billions of times. Conventional Monte Carlo integration is relatively inefficient for computing multidimensional integrals (or in the present work, sampling a multidimensional PDF), because samples are taken at random throughout the entire domain of the parameter space. Gregory (2005) provides the following illustration: suppose that for a one-parameter problem, the fraction of time spent sampling regions of high probability is 10^{-1}. Then in an M-parameter problem, this fraction could fall to 10^{-M}. In contrast, Markov chain Monte Carlo (MCMC) algorithms generate a Markov chain of samples (denoted by $\mathbf{m}^{(k)} \in \Re$; $\mathbf{m}^{(k)}$ is the kth sample) in proportion to the value of the PDF, so time is not wasted generating samples from regions in parameter space which contribute very little. More specifically, the MCMC method for sampling from a target PDF (e.g., posterior distribution) involves generating a stochastic (Markov) process whose stable distribution is the target PDF. Detailed theory and algorithms implementing the MCMC method are described by Hastings (1970), Gilks et al. (1996), Gregory (2005), among others. The Metropolis–Hastings algorithm is used for the present research.

Once a series of MCMC samples has been obtained, summary statistics related to each variable can be found. In the event that the target distribution is highly irregular (e.g., asymmetrical with multiple peaks or spikes), histograms are of descriptive value. In the present research, the mean is used as the summary statistic of choice, since the distributions encountered may be multiply peaked and irregular. In contrast, the maximum a posteriori estimator faces the potential problem of ignoring the bulk of the probability density by describing only an isolated local maximum.

3. Mock Urban Setting Test

The Mock Urban Setting Test (MUST) is a transport and dispersion experiment which took place at US Army Dugway Proving Ground in northern Utah during September 2001 (Yee and Biltoft, 2004). It was designed to simulate dispersion in a built-up (urban) area using an array of shipping containers (or building-like obstacles). This array consisted of 12 rows of obstacles in the streamwise x-direction and 10 columns in the spanwise z-direction. Propylene gas was used as a tracer and released from various locations within the array both continuously and near instantaneously, and concentration time series were obtained at detectors placed throughout the array. A physical model of the MUST field experiment was conducted at a scale of 1:205 in a boundary-layer water channel operated by Coanda Research & Development Corporation (Burnaby, British Columbia, Canada). A detailed description of the experiment is provided by Hilderman and Chong (2004) and Yee et al. (2006a). The inverse problem of source reconstruction is solved using individual concentration measurements D which are extracted from the concentration profiles that were measured during the water channel experiment.

The MUST array test case is useful for validating the source determination methodology because it possesses the following attributes:

(1) Detailed continuous source concentration data are available from a number of experiments at regularly-spaced locations within the array of obstacles.
(2) The experiments simulate an urban environment, which tests the ability of the methodology to locate a source lying in a built-up area.
(3) The flow encounters obstacles, which affect the expected shape of the posterior distribution (the probability of a source lying within a building is considered to be zero). Furthermore, obstacles induce recirculation zones, which enhance the mixing of the tracer and obscure the results of the inference procedure (i.e., the uncertainty of the source location is increased in these zones).

3.1. Procedure

3.1.1. C^* field generation

The C^* fields relevant to the MUST array are generated by solving the steady-state adjoint

advection-diffusion Eq. (26). The mean fluid velocities **u** are generated on a structured grid of points for the entire array using the urbanSTREAM code of Lien et al. (2005a, 2006). In order to reduce the computational workload, however, the adjoint code is only solved over a three-row subset of the domain. This domain size is sufficient, given that the bulk flow is in the x-direction and the plume width is smaller than the spanwise (z-direction) width of the domain. Fig. 3 shows an x–z slice of the mesh used for calculation of the C^* fields, with obstacles added to provide context.

Note that the mesh is significantly more dense between the first two rows of obstacles—this is a remnant of the fact that this mesh was originally designed for a forward dispersion calculation (the tracer was released from the region between the first two rows of buildings), and was not redesigned to accomodate the adjoint (backwards) calculations.

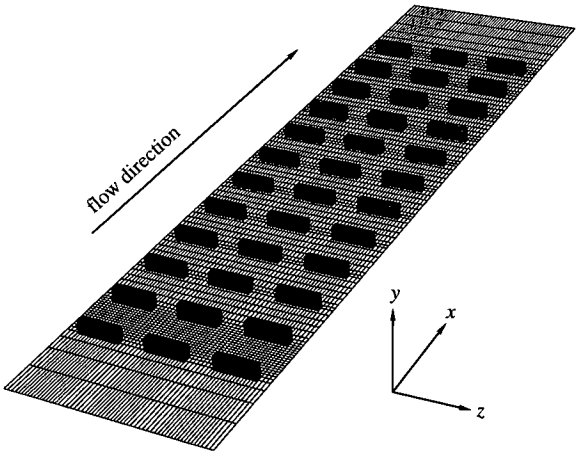

Fig. 3. A ground-level ($y = 0$) slice of the mesh on which the adjoint advection-diffusion equation was solved.

The C^* fields generated by the adjoint advection–diffusion code do not depend on time because the statistics of the velocity field (and, more particularly, the mean velocity) are stationary, and this example involves only a continuous release of tracer. However, the flow statistics are inhomogeneous in all three spatial directions, so one C^* field must be generated for each detector.

3.1.2. Detector selection

Concentration profiles were experimentally measured at several x-locations and heights. Fig. 4 shows an array of detector locations which lie along the paths of the experimental profiles. Starting from the left ($x = 0$), each spanwise line of detectors is numbered according to its position relative to the leftmost spanwise line of obstacles. The convention used here is to refer to the lines of detectors as belonging to rows 2.5, 3.5, 4.5, 6.5, 9.5 and 12.5. Experimental concentration profiles are not available at other x-locations.

By comparing the profiles generated by the forward dispersion model to the experimental profiles, it is clear that the model error dominates the measurement error. This comparison is shown for rows 2.5 and 4.5 in Fig. 5. Although the detector concentrations obtained using the C^* fields agree well with the forward dispersion model (as demanded by the duality relationship), the plume centerline concentration is increasingly overpredicted with increasing x-distance when compared with the experimental data. The lumped theoretical and measurement uncertainties for each detector, $\sigma_{L,i} = (\sigma_{D,i}^2 + \sigma_{T,i}^2)^{1/2}$, are assigned values based on these observed trends in the predictive accuracy of the dispersion model. These values lie between 10% and 270% of the mean concentration measured at a

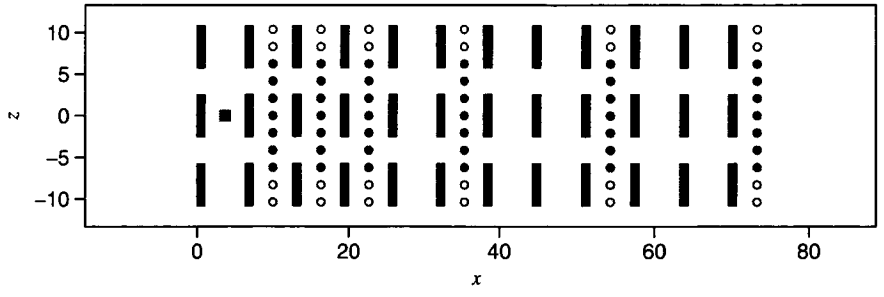

Fig. 4. MUST array source and detector configuration. The x, y, and z coordinates are normalized by the width of an obstacle in the streamwise (or, x) direction. The source (marked by the square) lies at ground level while the detectors (marked by circles) lie at $y = 0.5$ building heights in rows 2.5, 3.5, 4.5, 6.5, 9.5, and 12.5. In the spanwise direction, the detectors are placed at $z = 0.0$, ± 2.075, ± 4.150, ± 6.225, ± 8.305, ± 10.380 building heights. The filled circles depict the 42 detectors used to determine the source location.

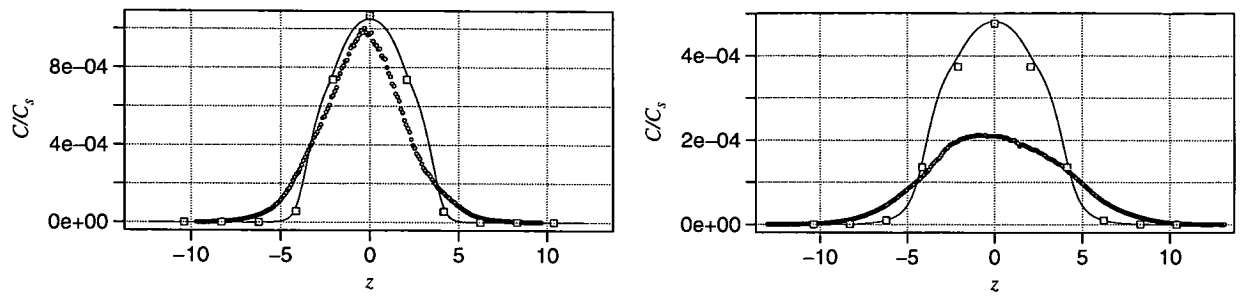

Fig. 5. Concentration profiles normalized by the source concentration C_s. Small circles represent experimental measurements, the solid line represents the solution to the forward advection–diffusion equation, and the squares represent detector concentrations reconstructed using C^* fields according to Eq. (27). (a) Concentration profile at row 2.5 and (b) concentration profile at row 4.5.

given detector. The 42 detector locations depicted in Fig. 4 were chosen as measurement stations to be used for the source reconstruction.

3.2. Results

The source reconstruction was performed using experimentally measured concentration data. The Metropolis-Hastings algorithm was used to generate 10^7 MCMC samples from various initial conditions. Since the acceptance rate (the proportion of accepted proposals out of the total number of samples drawn) was low (approximately 15%), these chains were thinned to obtain smaller chains consisting of every 100th sample in order to avoid autocorrelation (viz., to obtain approximately independent samples from the Markov chain). Although the chain was qualitatively found to quickly converge to the area of interest, we conservatively chose to discard the first half of these samples to avoid 'burn-in'. After discarding samples to avoid burn-in and thinning the Markov chain, the remaining 5×10^4 samples were used to generate the histograms shown in Fig. 6. It should be noted that the burn-in period is often chosen by inspecting the results of the Markov chain in order to determine whether it has reached a stationary distribution. The thinning interval can be selected by computing the autocorrelation function of the chain samples. Automatic methods for determining optimal burn-in and thinning parameters have been proposed in the MCMC literature (Gilks et al., 1996; Dunkley et al., 2005). In order to verify the MCMC results, the posterior distribution was evaluated directly, and the marginal distribution of each source parameter was obtained by numerically integrating the full posterior distribution over the remaining source parameters. The marginal distributions are also shown in Fig. 6. The stair-step appearance of the marginal x_s, y_s, z_s distributions is a remnant of the fact that the value of the distribution is only calculated at the center of each cell in the computational grid, and is not linearly interpolated at points in between. This appearance is not present in the graph for the q_s parameter because it is not considered discrete by the MCMC algorithm.

The marginal distribution corresponding to the streamwise source location, x_s, is obtained by integrating the full posterior PDF according to:

$$\begin{aligned} P(x_s|D,I) &= \int_{\text{all } y_s}\int_{\text{all } z_s}\int_{\text{all } q_s} P(x_s,y_s,,z_s,q_s|D,I) \\ &\quad \times \mathrm{d}y_s\,\mathrm{d}z_s\,\mathrm{d}q_s \\ &\approx \sum_{j=1}^{N_y}\sum_{k=1}^{N_z}\sum_{l=1}^{N_q} P(x_s,y_{s,j},z_{s,k},q_{s,l}|D,I) \\ &\quad \times \Delta y_s \Delta z_k \Delta q_l, \end{aligned} \tag{28}$$

where the grid cell dimensions Δx_s, Δy_s, Δz_s vary in space, but Δq_s is held constant. The marginal distributions for the other parameters are found similarly. The agreement between the MCMC results and the marginal distributions is good; small discrepancies are due to the parameter domain discretization used for the numerical integration.

The results shown in Fig. 6 demonstrate that the Bayesian methodology provides an honest assessment of the source-receptor relationship in that the source strength is underpredicted based on the available experimental concentration data and the performance of the dispersion model. The modelled concentrations near the centerline generally overpredict the measured concentrations and this is

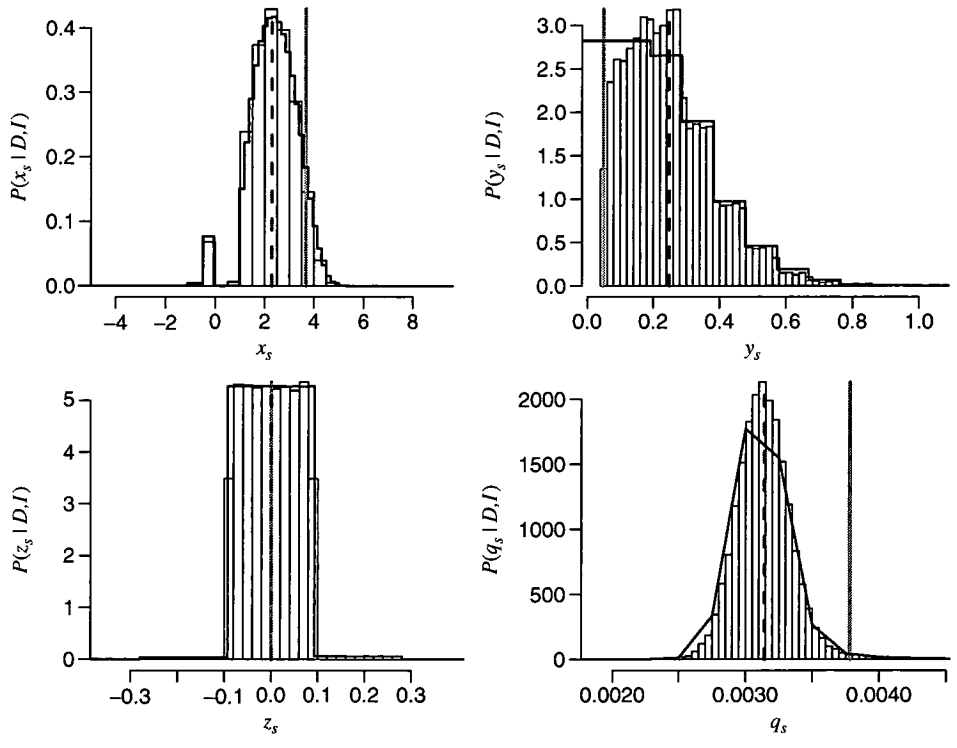

m_i	x_s	y_s	z_s	q_s
actual m_i	3.665	0.05	0.0	3.780×10^{-3}
mean(m_i^{MCMC})	2.294	0.248	0.001	3.141×10^{-3}
mean(m_i^{direct})	2.315	0.198	0.001	3.124×10^{-3}
sd(m_i^{MCMC})	1.127	0.134	0.060	2.123×10^{-4}
sd(m_i^{direct})	1.227	0.135	0.025	2.190×10^{-4}

Fig. 6. Marginal parameter distributions and summary statistics (mean and standard deviation) generated from both MCMC samples and direct marginalization of the posterior PDF. The histograms are generated from MCMC samples and the solid lines are generated using a direct calculation of the posterior distribution. The solid vertical line represents the true parameter value, and the dashed line is the mean of the MCMC samples. The parameter q_s was non-dimensionalized based on the flow rate, reference length, and reference velocity associated with the experiment.

reflected in the fact that the methodology expects the source to be of lesser strength. The source position in the spanwise coordinate, z_s, is very well resolved, as the bulk of the probability mass lies in the width of a single cell of the computational grid. This is an ideal result because the C^* fields are not linearly interpolated, so the value of the marginal posterior distribution does not change within a single cell for a fixed source strength q_s. It is also interesting to note that the x_s and y_s histograms are "smeared" across most of the length and height of the obstacle in the wake region between the first and second rows of the array, respectively. This demonstrates that the rapid mixing of the plume material in this region serves to obscure the source location, leading to an erosion in the quality of the inference.

4. Joint Urban 2003 atmospheric dispersion study

Mean concentration data were obtained at locations in and around downtown Oklahoma City, Oklahoma, US, during the Joint Urban 2003

atmospheric dispersion study which was conducted from 28 June 2003 to 31 July 2003 (Allwine et al., 2004). A sulfur hexafluoride (SF_6) tracer was released continuously for 30 min and sampled at a number of locations within the central business district of the city. For the present case, we used nine sampler sites to perform the source reconstruction. Fig. 7 shows the source and sampler locations with respect to the buildings present in the flow field. The dark contours surrounding the source (the area magnified in Fig. 8) represent the marginal posterior distribution for (x_s, y_s), obtained using direct evaluation of the full posterior PDF.

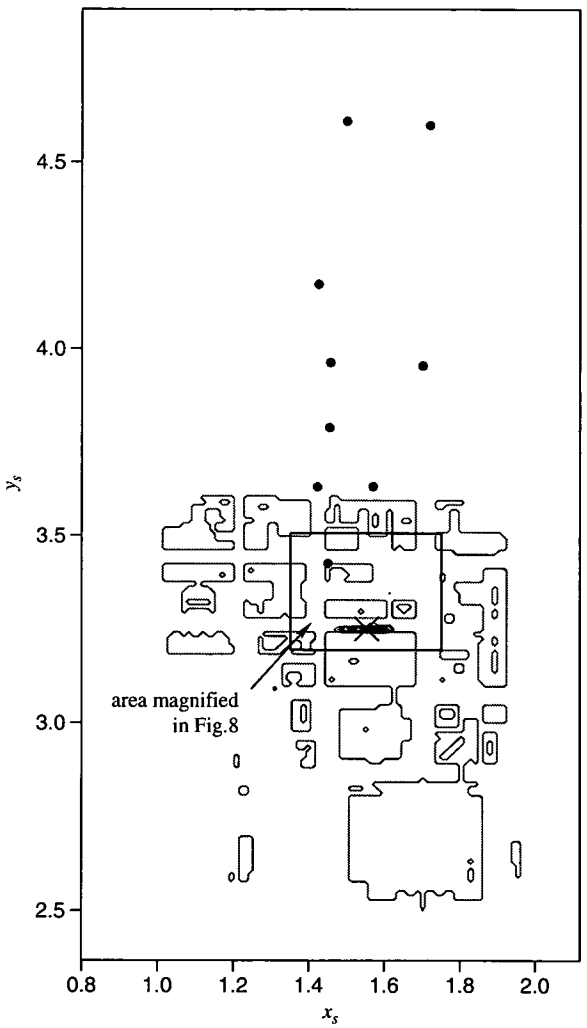

Fig. 7. Overhead view of the buildings (light contours), source (cross) and detectors (circles) for Oklahoma City. The dark contours represent the marginal posterior distribution $P(x_s, y_s|D, I)$. The prevailing wind direction is aligned with the positive y-axis. A magnification of the area surrounding the source is shown in Fig. 8.

Before solving the inverse problem, the wind field was found for the domain shown in Fig. 7 using the urbanSTREAM code of Lien et al. (2005a, 2006). The domain was subdivided into $98 \times 138 \times 68$ grid cells in the x, y, z directions, with the most refined cells located in the built-up area. The buildings in this area were explicitly resolved, while outside this area, a 'virtual' buildings approach was used to simulate the effect of buildings on the flow by introducing a drag-force term into the spatially-averaged mean momentum equation (Lien et al., 2005b). For each detector location, the adjoint advection-diffusion equation was solved, resulting in a set of nine C^* fields. The problem is steady-state, so the wind field statistics do not change with time, and the source height (z-location) is assumed known. The units of distance in the x and y directions correspond to the system of units used internally by the flow solver, and the source strength q_s is measured in grams per second.

Detector measurements from the experiment were used for the D_i, and the model and measurement uncertainties were assigned realistic quantities based on the ability of the forward and adjoint dispersion simulations to correctly predict the detector concentrations. Depending on the detector, these uncertainties typically range from 2% to 70% of the mean concentration measured at the detector.

4.1. Results

In Fig. 8, the distribution of MCMC samples (x_s^{MCMC}, y_s^{MCMC}) is plotted as a set of points in

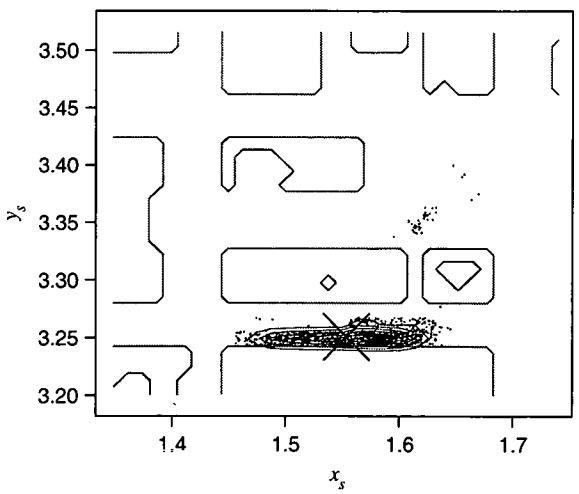

Fig. 8. Close-up view of the marginal $P(x_s, y_s|D, I)$ contours, overlaid on the MCMC samples (dots).

contrast with a two-dimensional contour map of the marginal (x_s, y_s) distribution. The points occasionally stray from the bulk of the probability mass outlined by the contours, which is an indication that the Markov chain experiences difficulty traversing regions of very low probability, i.e., through buildings. In this case, it is necessary to manually adjust MCMC algorithm parameters (e.g., increase the width of the proposal distribution) in order to encourage the chain to behave in a more exploratory fashion.

Both the MCMC histograms and marginal posterior distributions of the source parameters are shown in Fig. 9. The parameter estimates are shown in the table of Fig. 9. A one standard deviation interval about the estimated source parameters is seen to contain the true value of these parameters. In contrast to the MUST array case, the streamwise source coordinate y_s is well-estimated, with the bulk of the probability mass lying in the two grid cells which surround the source.

5. Conclusions

Bayesian probability theory has been successfully applied to solve the problem of source determination in a flexible and consistent way. By using the adjoint advection–diffusion equation along with MCMC sampling, calculations which yield an accurate picture of the full posterior distribution for the source parameters can be performed in a reasonable amount of time. Using these two techniques, the computational effort required for a fixed spatial domain size scales linearly with both the number of detectors and the number of source parameters. Without the adjoint approach, the computational effort would be proportional to the number of possible source locations, which is typically far greater than the number of detectors. Without using MCMC, the time required to sample from or directly evaluate the posterior PDF grows as a power of the dimensionality of the source parameters. The methodology is capable of simultaneously inferring at least four separate source parameter values: the location and strength are generally well estimated. The quality of the inference truthfully reflects the quality (in terms of the uncertainty) of the modelled and measured concentration data.

The primary source of the model uncertainty is our limited understanding of the physics of turbulent flows. Improving the turbulence-modelling

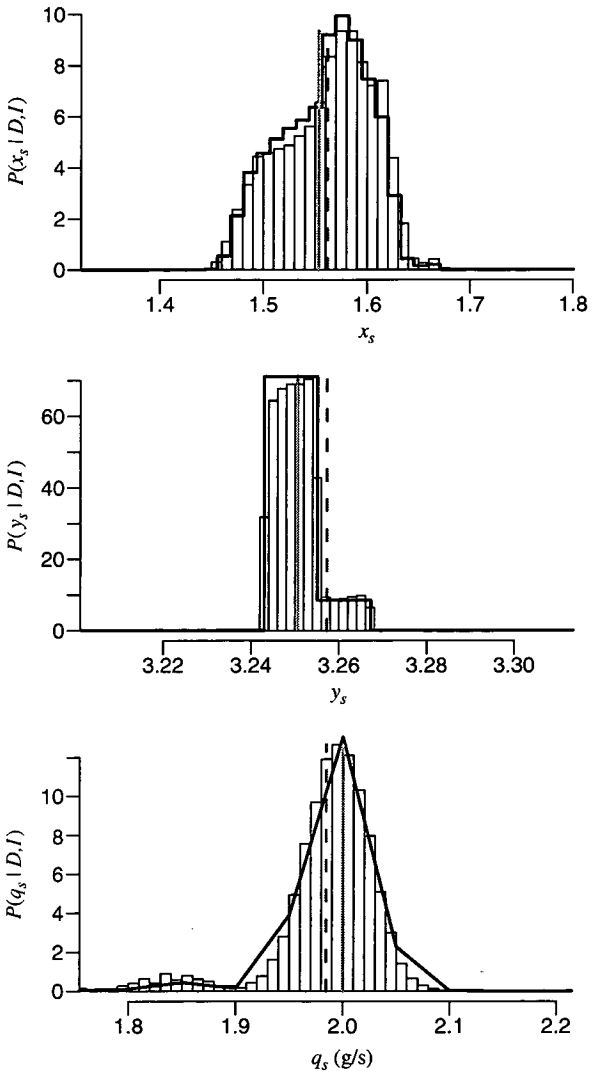

m_i	x_s	y_s	q_s (g/s)
actual m_i	1.554	3.251	2.0
mean(m_i^{MCMC})	1.562	3.257	1.985
mean(m_i^{direct})	1.559	3.254	1.990
sd(m_i^{MCMC})	0.044	0.025	0.049
sd(m_i^{direct})	0.042	0.019	0.041

Fig. 9. Source parameter estimates as determined using MCMC (histograms) and direct calculation of the marginal posterior distributions (dark lines). The true parameter value is shown by the solid vertical line, and the mean of the MCMC samples [mean(m_i^{MCMC})] is shown by the dashed line.

component of the flow solver and dispersion model would significantly improve the determination of the source location through a reduction in the discrepancy between the model dispersion predictions and the measured detector data.

Both of the test cases considered involve dispersion in built-up areas and demonstrate the utility of the method for practical applications in emergency and environmental management. Generating the flow field is by far the greatest computational burden, and adding the ability to perform source determination to computational fluid dynamics models for prediction of flow and dispersion in an urban environment does not increase this burden significantly.

Acknowledgements

The authors wish to acknowledge support from the Chemical Biological Radiological Nuclear Research and Technology Initiative (CRTI) Program under project number CRTI-02-0093RD.

References

Allwine, K.J., Clawson, K.L., Leach, M.J., Burrows, D., Wayson, R., Flaherty, J., Allwine, E., 2004. Urban dispersion processes investigated during the Joint Urban 2003 study in Oklahoma City. In: Fifth Conference on Urban Environment, Vancouver, British Columbia, Canada.

Aral, M.M., Guan, J., Maslia, M.L., 2001. Identification of contaminant source location and release history in aquifers. Journal of Hydrologic Engineering 6, 225–234.

Chow, T.K., Kosovic, B., Chan, S., 2005. Source inversion for contaminant plume dispersion in urban environments using building resolving simulations. In: Ninth Annual George Mason University Conference on Atmospheric Transport and Dispersion Modeling, Fairfax, VA, USA.

Cox, R.T., 1946. Probability, frequency and reasonable expectation. American Journal of Physics 14, 1–13.

Dunkley, J., Bucher, M., Ferreira, P.G., Moodley, K., Skordis, C., 2005. Fast and reliable MCMC for cosmological parameter estimation. Monthly Notices of the Royal Astronomical Society 356, 925–936.

Estep, D., 2004. A short course on duality, adjoint operators, Green's functions, and a posteriori error analysis. Course notes, Department of Mathematics, Colorado State University, ⟨http://www.math.colostate.edu/~estep/research/preprints/adjointcourse_final.pdf⟩.

Flesch, T.K., Wilson, J.D., Yee, E., 1995. Backward-time Lagrangian stochastic dispersion models and their application to estimate gaseous emissions. Journal of Applied Meteorology 34, 1320–1332.

Geer, L.-E.D., 1996. Sniffing out clandestine tests. Nature 382, 491–492.

Gilks, W.R., Richardson, S., Spiegelhalter, D.J. (Eds.), 1996. Markov Chain Monte Carlo in Practice. Chapman & Hall/CRC, London.

Goyal, A., Small, M.J., von Stackelberg, K., Burmistrov, D., Jones, N., 2005. Estimation of fugitive lead emission rates from secondary lead facilities using hierarchical Bayesian models. Environmental Science and Technology 39, 4929–4937.

Gregory, P.C., 2005. Bayesian Logical Data Analysis for the Physical Sciences: A Comparative Approach with *Mathematica*® support. Cambridge University Press, Cambridge.

Hastings, W.K., 1970. Monte Carlo sampling methods using Markov chains and their applications. Biometrika 57, 97–109.

Hilderman, T., Chong, R., 2004. A laboratory study of momentum and passive scalar transport and diffusion within and above a model urban canopy—MUST Array report. Report CRDC00327c, Prepared by Coanda Research and Development Corporation for Defence Research and Development Canada, Suffield.

Hourdin, F., Issartel, J.-P., 2000. Sub-surface nuclear tests monitoring through the CTBT xenon network. Geophysical Research Letters 27, 2245–2248.

Hsieh, K.J., Keats, W.A., Lien, F.-S., Yee, E., 2005. Scalar dispersion and inferred source location in an urban canopy. In: Ninth Annual George Mason University Conference on Atmospheric Transport and Dispersion Modeling, Fairfax, VA, USA.

Jaynes, E.T., 2003. Probability Theory: The Logic of Science. Cambridge University Press, Cambridge.

Jeremić, A., Nehorai, A., 2000. Landmine detection and localization using chemical sensor array processing. IEEE Transactions on Signal Processing 48, 1295–1305.

Keats, W.A., Lien, F.-S., Yee, E., 2006. Source determination in built-up environments through Bayesian inference with validation using the MUST Array and Joint Urban 2003 tracer experiments. In: CFD Society of Canada, 14th Annual Conference of Computational Fluid Dynamics, Kingston, Ont., Canada.

Kosovic, B., Sugiyama, G., Chow, T.K., Dyer, K., Hanley, W., Johannesson, G., Larsen, S., Loosmore, G., Lundquist, J.K., Mirin, A., Nitao, J., Serban, R., Tong, C., 2005. Stochastic source inversion methodology and optimal sensor network design. In: Ninth Annual George Mason University Conference on Atmospheric Transport and Dispersion Modeling, Fairfax, VA, USA.

Lien, F.-S., Yee, E., Ji, H., Keats, W.A., Hsieh, K.-J., 2005a. Development of a high-fidelity numerical model for hazard prediction in the urban environment. In: CFD Society of Canada, 13th Annual Conference of Computational Fluid Dynamics, St. John's, Newfoundland, Canada.

Lien, F.-S., Yee, E., Wilson, J.D., 2005b. Numerical modelling of the turbulent flow developing within and over a 3-D building array, Part II: a mathematical foundation for a distributed drag force approach. Boundary-Layer Meteorology 114, 245–285.

Lien, F.-S., Yee, E., Ji, H., Keats, A.K., Hsieh, K.J., 2006. Progress and challenges in the development of physically based numerical models for prediction of flow and contaminant dispersion in the urban environment. International Journal of Computational Fluid Dynamics (in press).

Lin, C.-H., Chang, L.-F.W., 2002. Relative source contribution analysis using an air trajectory statistical approach. Journal of Geophysical Research 107, 4583–4592.

Matthes, J., Gröll, L., Keller, H.B., 2005. Source localization by spatially distributed electronic noses for advection and diffusion. IEEE Transactions on Signal Processing 53, 1711–1719.

Michalak, A.M., Kitanidis, P.K., 2003. A method for enforcing parameter nonnegativity in Bayesian inverse problems with an application to contaminant source identification. Water Resources Research 39, 1033.

Nehorai, A., Porat, B., Paldi, E., 1995. Detection and localization of vapor-emitting sources. IEEE Transactions on Signal Processing 43, 243–253.

Pudykiewicz, J.A., 1998. Application of adjoint tracer transport equations for evaluating source parameters. Atmospheric Environment 32, 3039–3050.

Rapley, R., Robins, P., Thomas, P.A., 2005. Source term estimation and probabilistic sensor modelling. In: Ninth Annual George Mason University Conference on Atmospheric Transport and Dispersion Modeling, Fairfax, VA, USA.

Robertson, L., 2004. Extended back-trajectories by means of adjoint equations. Report RMK No.105, Swedish Meteorological and Hydrological Institute.

Skiba, Y.N., 2003. On a method of detecting the industrial plants which violate prescribed emission rates. Ecological Modelling 159, 125–132.

Sohn, M.D., Reynolds, P., Singh, N., Gadgil, A., 2002. Rapidly locating and characterizing pollutant releases in buildings. Journal of the Air and Waste Management Association 52, 1422–1432.

Wilson, J.D., Shum, W.K.N., 1992. A re-examination of the integrated horizontal flux method for estimating volatilisation from circular plots. Agricultural and Forest Meteorology 57, 281–295.

Yee, E., 2006. A Bayesian approach for reconstruction of the characteristics of a localized pollutant source from a small number of concentration measurements obtained by spatially distributed "Electronic Noses". Russian-Canadian Workshop on Modeling of Atmospheric Dispersion of Weapon Agents, Moscow, Russia.

Yee, E., Biltoft, C.A., 2004. Concentration fluctuation measurements in a plume dispersing through a regular array of obstacles. Boundary-Layer Meteorology 111, 363–415.

Yee, E., Gailis, R.M., Hill, A., Hilderman, T., Kiel, D., 2006a. Comparison of wind tunnel and water channel simulations of plume dispersion through a large array of obstacles with a scaled field experiment. Boundary-Layer Meteorology, in press, doi:10.1007/s10546-006-9084-2, 44pp.

Yee, E., Lien, F.-S., Keats, W.A., Hsieh, K.J., D'Amours, R., 2006b. Validation of Bayesian inference for emission source distribution reconstruction using the Joint Urban 2003 and European Tracer experiments. In: Fourth International Symposium on Computational Wind Engineering (CWE2006), Yokohama, Japan.

#527312
CA029100